An Evolutionary Approach to Lane Markings Detection in Road Environments

M. Bertozzi, A. Broggi, A. Fascioli, A. Tibaldi
Dipartimento di Ingegneria dell'Informazione
Università di Parma
I-43100 Parma, Italy
{bertozzi,broggi,fascioli,tibaldi}@ce.unipr.it

Abstract.

This paper presents the application of an evolutionary technique to lane markings detection in road environments. The aim is the localization of the path in images acquired by a vision system installed on-board of a vehicle for driving assistance or automation purposes. The first step of the procedure is the removal of the perspective effect from the images. The resulting bird's eye view image is analyzed by means of *ant* agents able to locate the lane markings.

Results are compared against the ones obtained thanks to a deterministic approach.

1 Introduction

An autonomous intelligent vehicle has to perform a number of functionalities. Among them *Lane Detection* plays a basic role. A number of research groups has developed Lane Detection systems using artificial vision [1, 2, 3, 4].

The visual perception of the road environment is a challenging task: the knowledge of the lane position has to be extracted from visual patterns detected in the images. In the localization of specific features such as road markings painted on the road surface, basic problems have to be faced:

- shadows (projected by trees, buildings, bridges, or other vehicles) may produce artifacts onto the road surface, and thus alter the road texture;
- the system has to be robust enough to cope with situations where lane markings are worn and partly missing;
- the system should be enough flexible to adapt to different road environments.

This work presents an approach aimed at the identification of lane markings in road images by means of *collaborative autonomous agents*.

The action paradigm of the agents has been conceived on the basis of the behavior of real ants that seek for food: each ant has the task of exploring the world, locating food, and signalling to other ants the path toward food. Ant leave the nest and explore the world in a stochastic way.

When they find a place with food, they mark the path from the nest to that place with pheromone. Pheromone attracts other ants, swiftly leading them to food. In this way paths leading to regions rich of food will attract more and more ants. At the same time, pheromone evaporates as time passes, avoiding to mislead ants to old places where food is already exhausted or toward not enough profitable paths [5, 6, 7].

In this work, autonomous agents (the *ants*) explore the image seeking for lane markings (the food). Digital pheromone is used to mark best paths.

This paper is organized as follows: section 2 illustrates principles and data representation of the agent paradigm. Section 3 introduces the model involved with agents' supervision, while section 4 presents significant results and touches possible improvements of the system.

2 Lane detection algorithm

A camera installed onto the ARGO prototype vehicle [8] is used to obtain images of the road (see figure 1.a).

2.1 Pre-processing phase

The initial processing step is the removal of the perspective effect [9]. Thanks to the knowledge of the camera calibration and to the assumption of a flat road in front of the vehicle, pixel are remapped onto a new domain. Resulting images represent a bird's eye view of the road (see figure 1.b). In these images lane markings are nearly-vertical bright lines surrounded by a darker background. Hence, a specific adaptive filtering is used to extract quasi-vertical bright lines (see figure 1.c) [10, 8, 11].

The result is a binary image where overtrheshold pixels represent lane markings.

2.2 The motion domain

An evolutionary approach with a number of independent agents acting as lane markings trackers is used for detecting lane markings. Agents explore the resulting binary image and stochastically detect the markings. The idea derives from the *Ant Colony Optimization* meta-heuristic, devised to solve hard combinatorial optimization problems, originally inspired by the communication behavior of real ants [6].

The ants' motion domain $\mathcal{D}$ is the binary image obtained from the pre-processing phase: overthreshold pixels represent ant's food, namely a *food-field* mapping defined as $\mathcal{F} : \mathcal{D} \mapsto \{f_{\text{yes}}; f_{\text{no}}\}$. Initially, the pheromone level $\mathcal{P} : \mathcal{D} \mapsto [0..\mathbb{R}^+]$ is 0 for each element in $\mathcal{D}$. Anyway, $\mathcal{P}$ is continuously updated by ants, while $\mathcal{F}$ is constant during the processing.

The domain $\mathcal{D}$ is recursively explored by subsequent batches of ants. The first ant of the batch enters $\mathcal{D}$ from the bottom in a random position ($\mathbf{a} = (x_{\text{ant}}, y_{\text{ant}})$ with $y_{\text{ant}} = 0$). Since lane markings are nearly vertical lines, at each step, the ant performs a single pixel movement along the vertical axis toward the top end of the image. Thus vertical movements are fully deterministic, while horizontal movements are stochastically computed according to the rules described in the following paragraph.

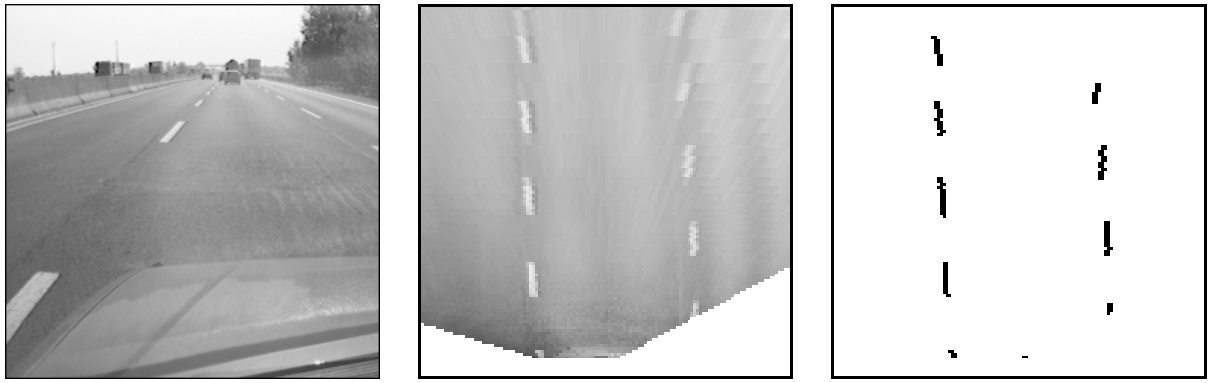

(a) (b) (c)

Figure 1: Initial steps of the processing: (*a*) original image, (*b*) removal of the perspective effect and (*c*) binary result.

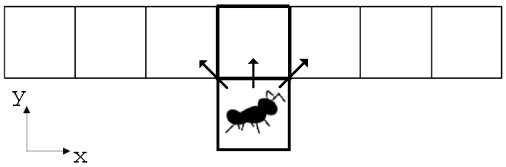

Figure 2: The $\mathcal{N}$ domain and possible ant's moves.

2.3 Evolutional algorithm

The horizontal position of an ant (x_{ant}) is modified according to values of $\mathcal{F}$ and $\mathcal{P}$ into sub-domain $\mathcal{N} \stackrel{\bullet}{=} \{\mathbf{a} \in \mathcal{D} \mid \quad y = 1 + y_{\text{ant}}, x_{\text{ant}} - \rho < x < x_{\text{ant}} + \rho\}$, where ρ represents the lateral field of view of each agent. In the current implementation of the algorithm $\rho = 3$ as shown in figure 2.

For each pixel $\mathbf{n} \in \mathcal{N}$ a quality parameter $w_{\mathcal{N}}(\mathcal{F}(\mathbf{n}), \mathcal{P}(\mathbf{n}))$ is computed as:

$$w_{\mathcal{N}} = \begin{cases} \alpha \times \mathcal{P}(\mathbf{n}) + \beta \times \mathcal{F}(\mathbf{n}) + \gamma \times (x_{\mathbf{n}} - x_{\text{ant}}) \times \mathcal{P}(\mathbf{n}) & \text{where} \quad \mathcal{F}(\mathbf{n}) = f_{\text{yes}} \wedge \mathcal{P}(\mathbf{n}) \neq 0 \\ 2 \times \alpha - 3 \times \gamma \times (x_{\mathbf{n}} - x_{\text{ant}}) & \text{where} \quad \mathcal{F}(\mathbf{n}) = f_{\text{yes}} \wedge \mathcal{P}(\mathbf{n}) = 0 \\ \alpha \times \mathcal{P}(\mathbf{n}) + \gamma \times (x_{\mathbf{n}} - x_{\text{ant}}) \times \mathcal{P}(\mathbf{n}) & \text{where} \quad \mathcal{F}(\mathbf{n}) = f_{\text{no}} \wedge \mathcal{P}(\mathbf{n}) \neq 0 \\ \begin{cases} 0 & \text{where} \quad |x_{\mathbf{n}} - x_{\text{ant}}| > 1 \\ 2 - |x_{\mathbf{n}} - x_{\text{ant}}| & \text{elsewhere} \end{cases} & \text{where} \quad \mathcal{F}(\mathbf{n}) = f_{\text{no}} \wedge \mathcal{P}(\mathbf{n}) = 0 \end{cases} \tag{1}$$

being α, β and γ empirically computed values.

The higher $w_{\mathcal{N}}$, the higher the pixel's *attraction* for ants. Therefore, an ant tends to *move left*, *stay in center*, or *move right* according to $w_{\mathcal{N}}$ belonging to pixels on the left side, in front, or on the right side respectively. More precisely, an attraction index (τ) for the three possible horizontal

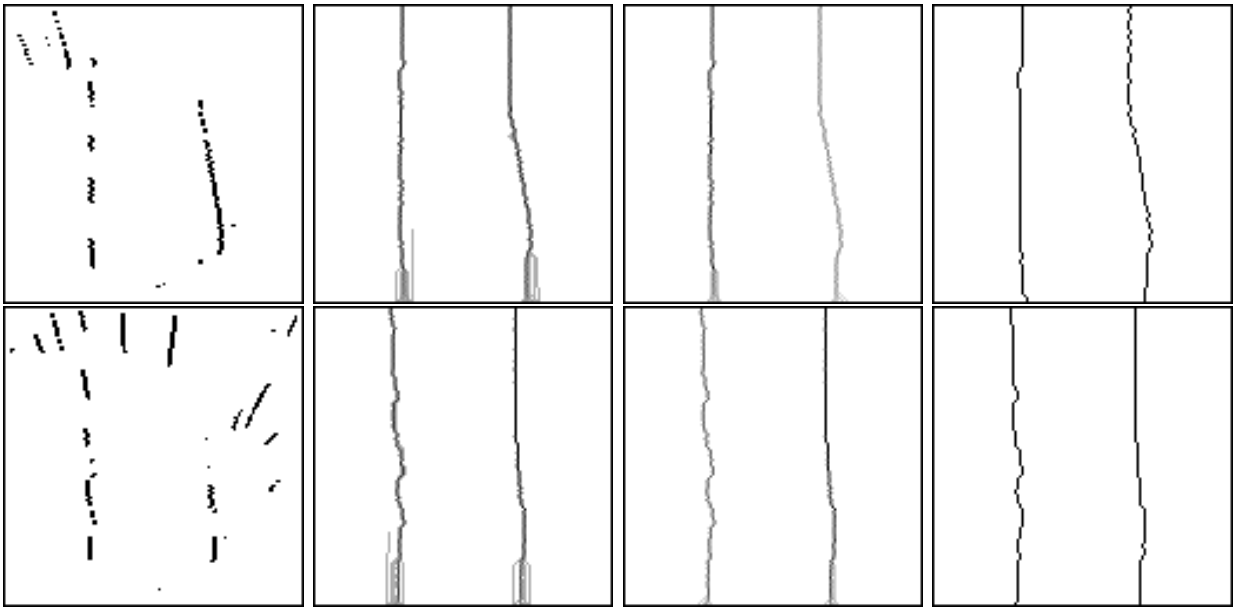

(a) (b) (c) (d)

Figure 3: Two examples of ants paths: (*a*) motion domain, (*b*) ant's presence level, (*c*) pheromone map $\mathcal{P}(\mathcal{D})$, and (*d*) detected markings.

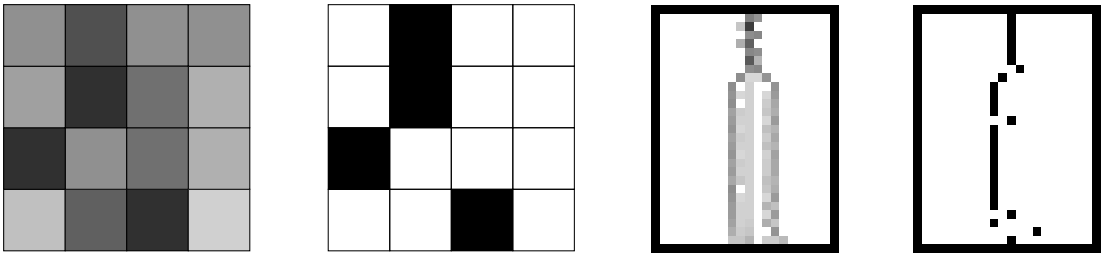

(a) (b) (c) (d)

Figure 4: Marking selection: (*a*) synthetic example of pheromone distribution, the darker the pixel the higher the pheromone value, (*b*) selected markings, namely pheromone maxima for (*a*), (*c*) real example of pheromone distribution and (*d*) selected markings for (*c*).

moves is computed as:

$$\begin{aligned} \tau_{\text{left}} &= \sum_{x_{\mathbf{n}} < x_{\text{ant}}} w_{\mathcal{N}}(\mathbf{n}) \\ \tau_{\text{center}} &= \sum_{x_{\mathbf{n}} = x_{\text{ant}}} w_{\mathcal{N}}(\mathbf{n}) \\ \tau_{\text{right}} &= \sum_{x_{\mathbf{n}} > x_{\text{ant}}} w_{\mathcal{N}}(\mathbf{n}) \end{aligned} \tag{2}$$

A truly random parameter u where $0 \leq \mathsf{u} \leq \tau_{\text{left}} + \tau_{\text{center}} + \tau_{\text{right}}$ is used to introduce a stochastic behavior in horizontal movements. When $u < \tau_{\text{left}}$ a left movement is chosen, when $\tau_{\text{left}} \leq u \leq \tau_{\text{left}} + \tau_{\text{center}}$ the central pixel is chosen, otherwise a right move is performed.

In order to speed up computation, invalid or scarce-food paths are immediately discarded: when an ant reaches lateral borders of $\mathcal{D}$ or when too many consecutive path's positions have $\mathcal{F} = f_{\text{no}}$,

```
foreach x ∈ D
    update F(x)
    reset P(x)
endfor
repeat following n̄ times
    foreach track in {left; right}
        update_starting_point(track)
        with every ants.v
            food_places_visited ← 0
            consecutive_empty ← 0
            path_length ← W
            k ← 0
            cycle row through {0..W}
                ant_step(a^k, F, P, track)
                path[k] ← a^k
                if F(a^k) = F_yes
                    increase empty_place_visited
                fi
                if on_lateral_border(a^k)
                    path_length ← row
                    next cycle break
                fi
                kill_path_if(consecutive_empty, food_places_visited)
                k ← k + 1
            endcycle
            max_food_places_visited max= food_places_visited
        endwith
        with every ants.v
            if food_places_visited = max_food_places_visited
                raise( P(path[*]) )
            fi
    endforeach
```

Figure 5: Main processing flow illustrated using a pseudo-language.

the ant is eliminated. This aspect is clearly evident in figure 3.b where ant's presence shows a number of ending paths.

The ant action performed during the step k has been implemented into the routine `ant_step( ... )`, summarized in figure 5.

2.4 Batch processing

When an ant reaches the top end of the image, another ant of the batch enters $\mathcal{D}$. At the end of the batch, the path of the ant that ran across the highest number of lane markings pixels is chosen as the best, and the pheromone level $\mathcal{P}$ of all of the pixels belonging to this path is increased by a unit.

Thanks to the iteration of this procedure on a number of batches, the attraction of the best paths becomes greater and greater. The number of ants that stepped over a pixel of $\mathcal{D}$ is shown in figure 3.b. Figure 3.c depicts the pheromone deposed at the end of the recognition phase.

As shown in figure 4, at the end of the image processing, the pixel representing the marking is selected for each row as the pixel that features the maximum of $\mathcal{P}(x)$, with x belonging to the row. No thinning procedure is needed, since for each row there is only a single maximum; on the other side, this approach does not guarantee that detected markings would be continuous (see figure 4.d).

Since the final target is to find the lane, thus both left and right markings, two different processings are performed for locating the left and the right lane markings, the only difference being the initial position of ants used for crossing $\mathcal{D}$. The assumption that the initial position of right and left markings is in the right and left half portion of $\mathcal{D}$ respectively is used. Ants used for detecting the left marking enter $\mathcal{D}$ in a random positions within an interval $\mathcal{E}_{\mathcal{D}}^{\text{left}}$ in the left portion of the image bottom. Analogously, the detection of the right marking starts from the right side of the bottom of $\mathcal{D}$ within the $\mathcal{E}_{\mathcal{D}}^{\text{right}}$ interval. The distance between left and right markings prevents the ants to reach the other marking allowing a reliable separate detection.

3 Lane tracking

At the beginning of the processing, the vision system is assumed to be centered inside the lane. Therefore entrance intervals $\mathcal{E}_{\mathcal{D}}^{\text{left}}$ and $\mathcal{E}_{\mathcal{D}}^{\text{right}}$ of ants batches are centered in given positions symmetrical with respect to the center of the image (see figure 6.a).

A simple tracking is performed in order to cope with lateral vehicle movements inside the lane and to take advantage of the high temporal correlation amongst subsequent frames. The assumption that the car is always oriented along the road direction is used and only slow lateral shifts and lane changes are considered. Strong correlation is then expected between position of markings in subsequent images.

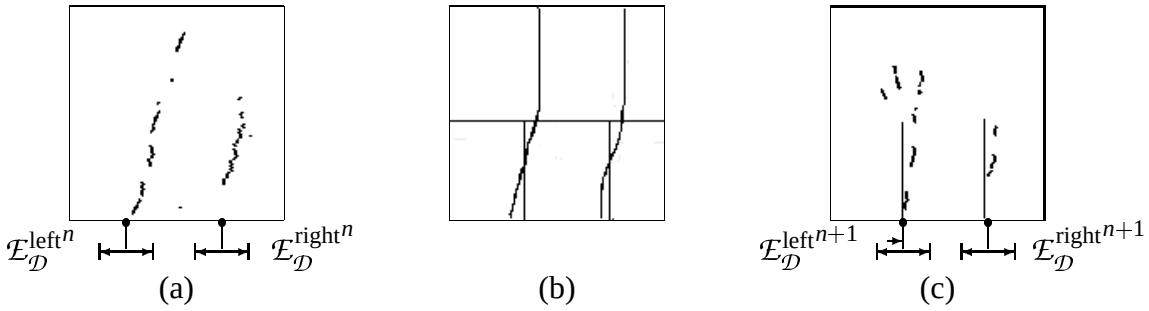

(a) (b) (c)

Figure 6: Update of entrance intervals: (*a*) initial position of intervals, (*b*) computation band used for determining the new position and (*c*) new intervals positions.

$\mathcal{E}_{\mathcal{D}}^{\text{left}}$ and $\mathcal{E}_{\mathcal{D}}^{\text{right}}$ are updated according to the result of the processing. The average value of left and right lane markings abscissa within a bottom band of $\mathcal{D}$ is computed (see figure 6.b). Resulting values for left and right markings are used to move $\mathcal{E}_{\mathcal{D}}^{\text{left}}$ and $\mathcal{E}_{\mathcal{D}}^{\text{right}}$ where next frame markings are supposed to be found (see figure 6.c). This mechanism allows to also cope with varying width lanes.

A more complex strategy is used when the driving system is executing a lane change. In such a case $\mathcal{E}_{\mathcal{D}}^{\text{left}}$ or $\mathcal{E}_{\mathcal{D}}^{\text{right}}$ move outside $\mathcal{D}$. When this event occurs, namely when the left or the right marking leaves the field of view, a new marking is supposed to enter the image from the opposite side. The new marking is searched for assuming the same width for different lanes. At each step the lane width W_l is computed as the average distance between $\mathcal{E}_{\mathcal{D}}^{\text{right}}$ and $\mathcal{E}_{\mathcal{D}}^{\text{left}}$ in the previous 5 frames. For example, when executing a left lane change, $\mathcal{E}_{\mathcal{D}}^{\text{left}}$ and $\mathcal{E}_{\mathcal{D}}^{\text{right}}$ move rightward until $\mathcal{E}_{\mathcal{D}}^{\text{right}}$ exits $\mathcal{D}$. Then $\mathcal{E}_{\mathcal{D}}^{\text{left}}$ is assumed as the new $\mathcal{E}_{\mathcal{D}}^{\text{right}}$, while a new $\mathcal{E}_{\mathcal{D}}^{\text{left}}$ is placed at distance W_l on the left.

4 Discussion

The system has been implemented and tested on an Athlon 1.3 GHz architecture using Linux. The whole processing can be carried out in 8.6 ms, namely at a 116 Hz rate without considering image acquisition.

The algorithm has been tested and proven to be robust in different conditions: without obstacles, on straight and curved roads, in different illumination conditions. Figure 7 shows a number of partial and final results of the processing. Figures 7.a and 7.b show the original image before and after the removal of the perspective effect, while figures 7.c and 7.d present the final result superimposed on 7.a and 7.b.

The most critical behavior corresponds to the absence of markings in presence of very strong curves and to the presence of vehicles that occlude markings. Figure 8 shows such a situation: the border of a marking-occluding vehicle is wrongly detected as the lane marking. Nevertheless, the misdetection only affects the portion of the image where no marking is detectable, while the visible portion of the marking is always correctly detected.

Figure 9 shows a comparison between the results obtained through this approach and the ones obtained by a previously developed fully-deterministic algorithm [11]. In particular, the most critical situation for the deterministic approach is the presence of obstacles occluding lane markings that could lead to the misdetection of the whole marking as shown in the first row of figure 9.a. Conversely, the new stochastic approach has evidenced not only a faster execution time in all conditions, but also a better precision and robustness even with differently positioned vehicles or obstacles. On the other side, ant's paths are less smooth than the ones deterministically computed. Anyway, an interpolation using high order functions is currently under implementation.

A more sophisticated lane tracking system is currently under development. The main idea is to bound the region in which ants can freely move according to the result of previous frames.

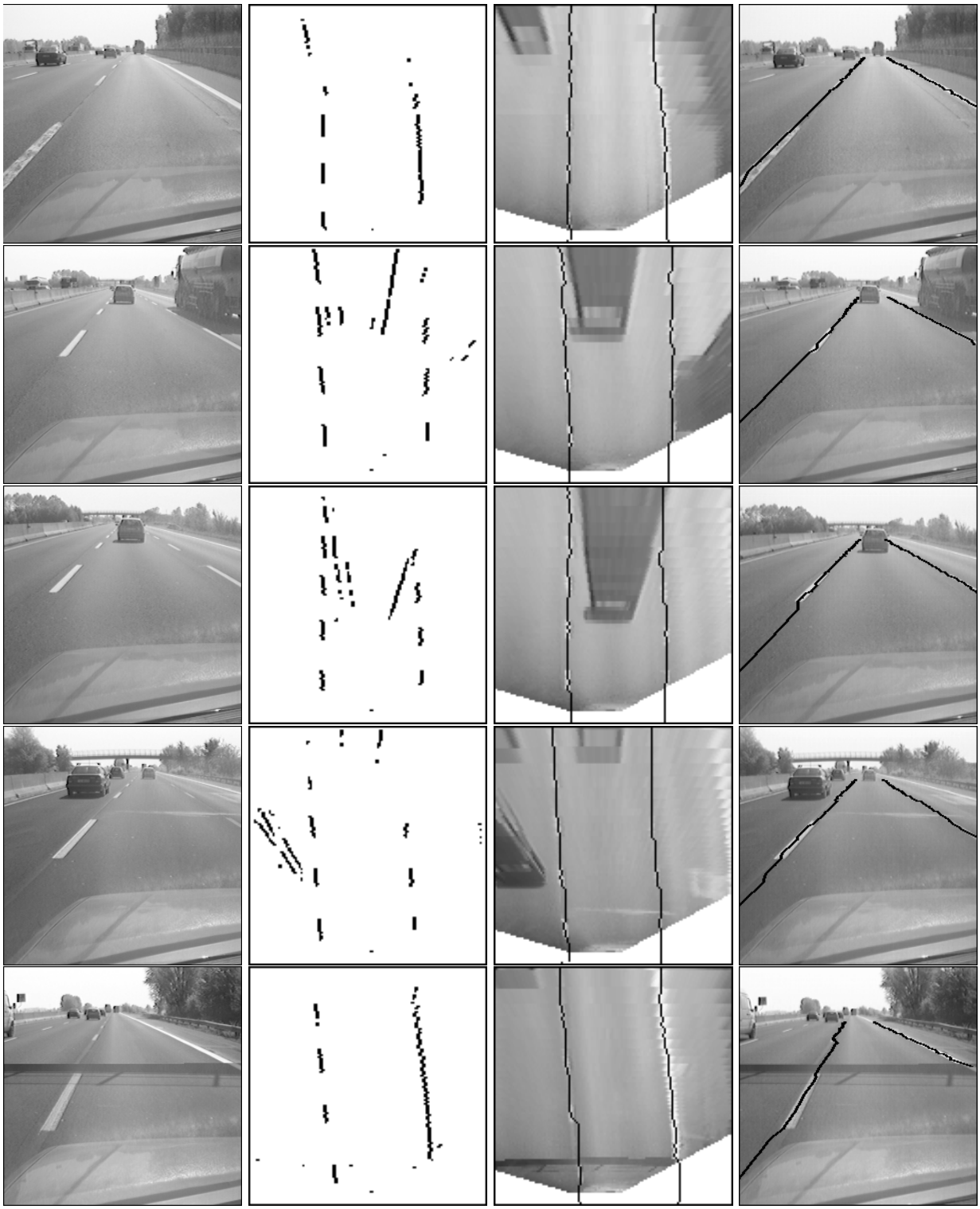

(a) (b) (c) (d)

Figure 7: Overview of the processing: (*a*) original image, (*b*) binarization after the removal of the perspective effect, (*c*) result superimposed on the image without the perspective effect and (*d*) results superimposed onto original image.

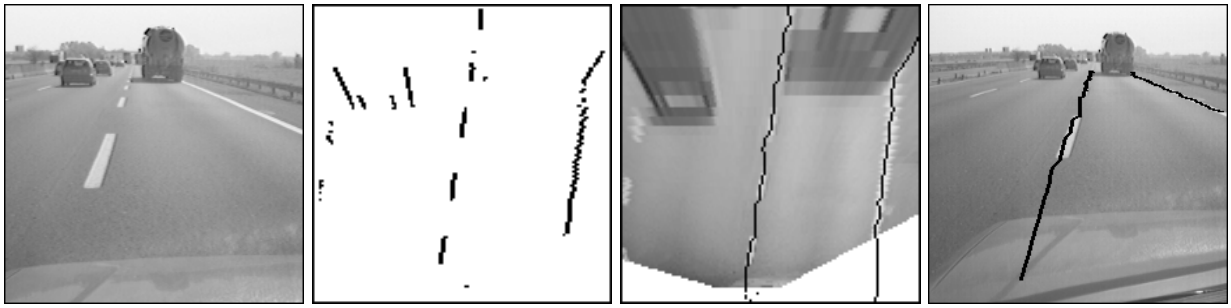

(a) (b) (c) (d)

Figure 8: Example of critical situation (occluding obstacle): (*a*) original image, (*b*) binarized, (*c*) result superimposed onto the image obtained by the removal of the perspective effect and (*d*) result superimposed onto original image.

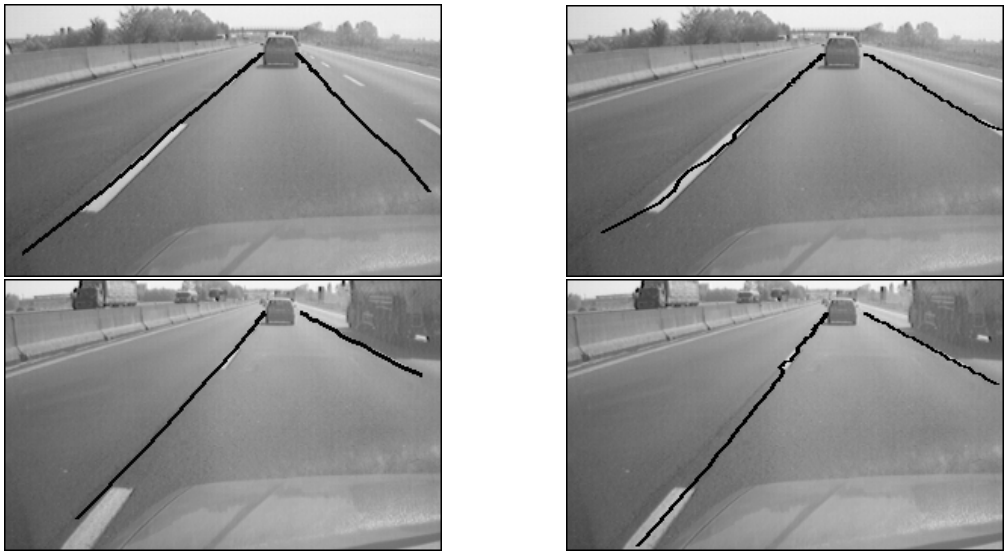

(a) (b)

Figure 9: Different approaches comparison: (*a*) results of the deterministic approach [11] and (*b*) results of the stochastic technique.

References

[1] J. D. Crisman and C. E. Thorpe, "UNSCARF, A Color Vision System for the Detection of Unstructured Roads," in *Procs. IEEE Intl. Conf. on Robotics and Automation*, (Sacramento, CA), pp. 2496–2501, Apr. 1991.

[2] S. L. Michael Beuvais, Chris Kreucher, "Building World Model for Mobile Platforms using Heterogeneous Sensors Fusion and Temporal Analysis," in *Procs. IEEE Intl. Conf. on Intelligent Transportation Systems'97*, (Boston, USA), p. 101, Nov. 1997.

[3] T. M. Jochem, D. A. Pomerleau, and C. E. Thorpe, "MANIAC: A Next Generation Neurally Based Autonomous Road Follower," in *Procs. 3rd Intl. Conf. on Intelligent Autonomous Systems*, (Pittsburgh, USA), Feb. 1993.

[4] D. A. Pomerleau and T. Jochem, "Rapidly Adapting Machine Vision for Automated Vehicle Steering," *IEEE Expert*, vol. 11, pp. 19–27, Apr. 1996.

[5] M. Bertozzi, A. Broggi, A. Fascioli, and P. Lombardi, "Vision-based Pedestrian Detection: will Ants Help?," in *Procs. IEEE Intelligent Vehicles Symposium 2002*, (Paris, France), June 2002. In press.

[6] M. Dorigo and G. Di Caro, "The ant colony optimization meta-heuristic," in *New Ideas in Optimization* (D. Corne, M. Dorigo, and F. Glover, eds.), pp. 11–32, London, UK: McGraw-Hill, 1999.

[7] M. Dorigo and L. M. Gambardella, "Ant Colony System: A Cooperative Learning Approach to the Traveling Salesman Problem," *IEEE Tran. on Evolutionary Computation*, vol. 1, pp. 53–66, Apr. 1997.

[8] A. Broggi, M. Bertozzi, A. Fascioli, and G. Conte, *Automatic Vehicle Guidance: the Experience of the ARGO Vehicle*. Singapore: World Scientific, Apr. 1999. ISBN 9810237200.

[9] M. Bertozzi, A. Broggi, and A. Fascioli, "Stereo Inverse Perspective Mapping: Theory and Applications," *Image and Vision Computing Journal*, vol. 8, no. 16, pp. 585–590, 1998.

[10] A. Broggi, M. Bertozzi, G. Conte, and A. Fascioli, "ARGO Prototype Vehicle," in *Intelligent Vehicle Technologies* (L. Vlacic, F. Harashima, and M. Parent, eds.), ch. 14, pp. 445–493, London, UK: Butterworth–Heinemann, June 2001. ISBN 0750650931.

[11] M. Bertozzi, A. Broggi, and A. Fascioli, "Visual Perception and Learning in Road Environments," in *Procs. 6th Intl. Conf. on Intelligent Autonomous Systems, IAS-6*, (Venice, Italy), pp. 885–892, July 2000.